



## RESEARCH ARTICLE

# Riparian buffers act as microclimatic refugia in oil palm landscapes

Joseph Williamson<sup>1</sup> | Eleanor M. Slade<sup>2</sup> | Sarah H. Luke<sup>3,4</sup> | Tom Swinfield<sup>5</sup> | Arthur Y. C. Chung<sup>6</sup> | David A. Coomes<sup>5</sup> | Herry Heroin<sup>7</sup> | Tommaso Jucker<sup>8</sup> | Owen T. Lewis<sup>9</sup> | Charles S. Vairappan<sup>7</sup> | Stephen J. Rossiter<sup>1</sup> | Matthew J. Struebig<sup>3</sup>

<sup>1</sup>School of Biological and Chemical Sciences, Queen Mary University of London, London, UK; <sup>2</sup>Asian School of the Environment, Nanyang Technological University, Singapore City, Singapore; <sup>3</sup>Durrell Institute of Conservation and Ecology (DICE), School of Anthropology and Conservation, University of Kent, Canterbury, UK; <sup>4</sup>Department of Zoology, University of Cambridge, Cambridge, UK; <sup>5</sup>Department of Plant Sciences, University of Cambridge Conservation Research Institute, Cambridge, UK; <sup>6</sup>Forest Research Centre, Sabah Forestry Department, Sandakan, Sabah, Malaysia; <sup>7</sup>Institute for Tropical Biology and Conservation, Universiti Malaysia Sabah, Kota Kinabalu, Sabah, Malaysia; <sup>8</sup>School of Biological Sciences, University of Bristol, Bristol, UK and <sup>9</sup>Department of Zoology, University of Oxford, Oxford, UK

**Correspondence**

Joseph Williamson  
Email: joseph.williamson@qmul.ac.uk

Stephen J. Rossiter  
Email: s.j.rossiter@qmul.ac.uk

**Funding information**

Newton-Ungku Omar Fund via the British Council and Malaysian Industry Government Group for High Technology, Grant/Award Number: 216433953; Natural Environment Research Council, Grant/Award Number: NE/K016261/1, NE/K016377/1, NE/L002485/1 and NE/S01537X/1

**Handling Editor:** Julio Louzada

**Abstract**

1. There is growing interest in the ecological value of set-aside habitats around rivers in tropical agriculture. These riparian buffers typically comprise forest or other non-production habitat, and are established to maintain water quality and hydrological processes, while also supporting biodiversity, ecosystem function and landscape connectivity.
2. We investigated the capacity for riparian buffers to act as microclimatic refugia by combining field-based measurements of temperature, humidity and dung beetle communities with remotely sensed data from LiDAR across an oil palm dominated landscape in Borneo.
3. Riparian buffers offer a cool and humid habitat relative to surrounding oil palm plantations, with wider buffers characterised by conditions comparable to riparian sites in continuous logged forest.
4. High vegetation quality and topographic sheltering were strongly associated with cooler and more humid microclimates in riparian habitats across the landscape. Variance in beetle diversity was also predicted by both proximity-to-edge and microclimatic conditions within the buffer, suggesting that narrow buffers amplify the negative impacts that high temperatures have on biodiversity.
5. *Synthesis and applications.* Widely legislated riparian buffer widths of 20–30 m each side of a river may provide drier and less humid microclimatic conditions than continuous forest. Adopting wider buffers and maintaining high vegetation quality will ensure set-asides established for hydrological reasons bring co-benefits for terrestrial biodiversity, both now, and in the face of anthropogenic climate change.

This is an open access article under the terms of the Creative Commons Attribution License, which permits use, distribution and reproduction in any medium, provided the original work is properly cited.

© 2020 The Authors. *Journal of Applied Ecology* published by John Wiley & Sons Ltd on behalf of British Ecological Society

**KEYWORDS**

agriculture, biodiversity, Borneo, climate change, habitat fragmentation, microclimate, riparian buffer, tropical forest

## 1 | INTRODUCTION

Microclimate determines how organisms interact with their surroundings, from development and physiology, to behaviour, ecology, function and distribution (Jucker et al., 2020). The need to understand how microclimate varies across land-use mosaics is acute in the wet tropics, where high biodiversity is threatened by the combined impacts of rapid land-use change and climatic warming (Travis, 2003). Fine-scale microclimate is shaped by multiple environmental factors, including solar radiation, wind, topography and vegetation structure (Helmuth, 2009). As such, microclimatic gradients are particularly pronounced across tropical agriculture-forest mosaics, where vegetation structure can vary dramatically (Blonder et al., 2018; Jucker et al., 2018). Degraded forests have higher temperatures and lower humidities than undisturbed forests (Hardwick et al., 2015), although both are cooler than farmland (Hardwick et al., 2015; Meijide et al., 2018; Silvério et al., 2015).

Riparian buffers, or riparian reserves, are areas of non-production habitat (often forest) retained around rivers in agricultural landscapes, primarily as a means of protecting water quality by reducing run-off (Tabacchi et al., 2000). In many tropical nations, riparian buffers of a designated width are required by law, often based on the size of the river in question (Luke, Slade, et al., 2019). In addition, policies on riparian buffer width have been adopted by groups such as the Roundtable on Sustainable Palm Oil (RSPO) as part of their certification criteria for mitigating the detrimental impacts of oil palm development on the environment and local communities (Luke, Slade, et al., 2019). In addition to their primary role in protecting water quality, riparian buffers provide a range of other ecosystem services, such as carbon storage (Mitchell et al., 2018), flood protection (Tabacchi et al., 2000) and subsidising water courses with terrestrially derived organic matter (Allan, 2004). Buffers can also provide co-benefits for a variety of terrestrial (Barlow et al., 2010; Keir et al., 2015; Zimbres et al., 2017) and aquatic taxa (Cunha & Juen, 2017; Giam et al., 2015). There are also examples of these habitat remnants serving as corridors between other forest areas, promoting connectivity for various taxa (Gray et al., 2019; Keuroghlian & Eaton, 2008).

In common with all habitat fragments, the efficacy of riparian buffers for safeguarding biodiversity and promoting connectivity will depend on habitat area and quality, the level of contrast with the surrounding matrix, and the biology of the taxa in question (Lees & Peres, 2008). In general, the attributes of riparian buffers that support terrestrial biodiversity remain poorly understood. Recent studies have demonstrated the role of buffer width for birds (Keir et al., 2015; Lees & Peres, 2008; Mitchell et al., 2018), mammals (Zimbres et al., 2017) and dung beetles (Barlow et al., 2010; Gray et al., 2017), with several subsequently linking observed biodiversity patterns to habitat quality (Lees & Peres, 2008; Mitchell et al., 2018).

However, studies investigating riparian buffer microclimates and the features that shape them are scarce (e.g. Nagy et al., 2015).

Insights into the effects of microclimate on tropical biodiversity are often limited by issues of scale and accuracy (Jucker et al., 2018; Schulze et al., 2001), with most studies relying on coarse-resolution mapping databases such as WorldClim (Fick & Hijmans, 2017). Advances in technologies such as Light Detection And Ranging (LiDAR) make it possible to map landscapes and vegetation with unprecedented levels of accuracy and precision (Zellweger et al., 2019), allowing studies to better quantify and link physical habitat structure to microclimate (Jucker et al., 2018). The decreasing costs of microclimatic dataloggers have also catalysed an increase in research investigating fine-scale microclimatic conditions (e.g. Hardwick et al., 2015; Law et al., 2019).

Here we combine information from airborne LiDAR with field-based microclimatic measurements to investigate the efficacy of forested riparian buffers of different widths and habitat composition for providing microrefugia within oil palm plantations. We deployed dataloggers across three riparian habitats: oil palm, riparian buffers and continuous logged-forest, in Sabah, Malaysian Borneo. First, we examine if riparian buffers in otherwise microclimatically extreme plantations maintain conditions similar to those found in continuous riparian forest. We then demonstrate how vegetation conditions and topography shape the microclimate within riparian buffers, and across human-modified landscapes as a whole, before evaluating how edge effects influence buffer microclimate and the implications this has for policy pertaining to buffer width. Finally, to assess the capacity of tropical riparian buffers to act as microrefugia for a key invertebrate indicator group (*Scarabaeinae*), we couple the microclimatic data with dung beetle community data across the modified landscape.

## 2 | MATERIALS AND METHODS

### 2.1 | Study site

Fieldwork was conducted in and around the Stability of Altered Forest Ecosystems project ([www.safeproject.net](http://www.safeproject.net); 4°81'N 117°25'E - 4°43'N 117°64'E, plot elevation ranged from 125 to 450 m a.s.l.) in Sabah, Malaysia (Northern Borneo, Figure 1a). This region is characterised by a tropical climate, with annual rainfall ~2,700 mm and a mean annual temperature of 26.7°C (Walsh & Newbery, 1999), although a recent study shows the region has become hotter and drier in recent years (Chapman et al., 2020). The area was formerly continuous lowland dipterocarp forest with much of the remaining forest having been selectively logged in the 1970s and 2000s, and subsequently salvage logged in 2013 and 2015 in preparation for oil palm (Struebig et al., 2013). At the time of fieldwork, this forest was highly fragmented, bounded to the north

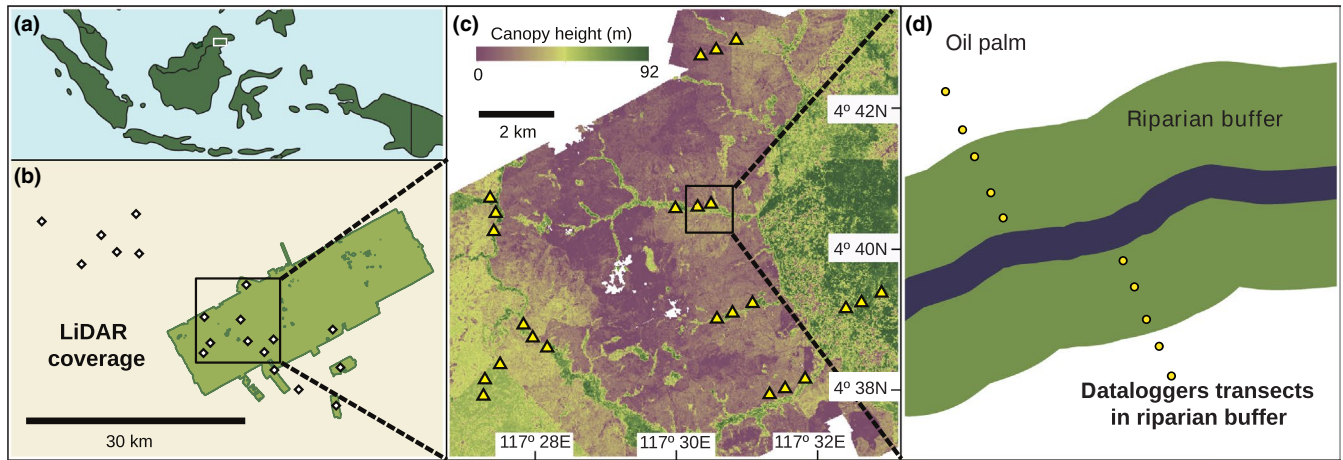


**FIGURE 1** Study location and design. (a) Map of Southeast Asia with panel B denoted by a white rectangle. (b) Study landscape with the green silhouette denoting the airborne LiDAR-scan area, and points denoting the 20 study rivers. A black square denotes the area shown in panel c. (c) LiDAR-derived canopy height model of part of our study landscape. Yellow triangles denote sampling transects ( $n = 60$ ). (d) Sampling design for a riparian buffer transect. Yellow circles denote datalogger points. Positions of dataloggers are (from river outwards) 5 m from the river, 15 m from the river, ~5 m from the buffer-oil-palm edge, 5 m into oil palm and 25 m into oil palm. The blue line denotes the river

by continuous forest, and surrounded by oil palm plantations (planted 8–12 years previously) elsewhere (Figure 1).

Between December 2016 and May 2018, we deployed dataloggers (EasyLog USB, Lascar Electronics) in 300 locations across 60 transects (5 dataloggers per transect) on 20 rivers (3 transects per river) in the landscape: in oil palm plantations (OP:  $n = 2$  rivers, 6 transects), riparian forest buffers within oil palm plantations (RB:  $n = 16$  rivers, 48 transects) and continuous logged forest (CF:  $n = 2$  rivers, 6 transects). Distances between adjacent transects on a river were 342–591 m, with rivers varying from 0.5 to 48 km apart (median 18 km). In oil palm and continuous forest, dataloggers were deployed in transects perpendicular to the riverbank at distances of 5, 15, 25, 35 and 45 m. In riparian buffer transects, dataloggers were deployed at 5 and 15 m from the riverbank and at ~5 m from the buffer-oil-palm edge, and at 5 and 25 m into the oil palm (Figure 1d). A range of buffer widths (0–324 m) were investigated to investigate the effect of proximity-to-edge on microclimate. All units were suspended at 3 m above the ground with a polystyrene plate rain-cover and left to record temperature ( $T$ , °C) and relative humidity (RH, %) for 3–7 weeks at intervals of 30 min.

## 2.2 | Microclimate data

Datalogger data were collated to calculate maximum ( $T_{\max}$ ) and mean ( $T_{\text{mean}}$ ) daily temperatures for each sampling day. RH was used to calculate vapour pressure deficit (VPD, hPa) - the difference in the partial pressure of water vapour in the air compared with saturated air at a given temperature ( $T$ ):

$$\text{VPD} = \frac{100 - \text{RH}}{100} e_s, \text{ where } e_s = 6.112e^{\frac{17.67T}{T+243.5}}$$

Vapour pressure deficit represents the evaporative demand of the air, pulling water up through the soil-root-stem-leaf continuum. Thus, it is a critical determinant of plant ecology, strongly influencing potential

evapotranspiration and the ability of plants to supply their leaves with sufficient water during the driest parts of the day, and thereby regulating seedling growth and mortality (Williams et al., 2013). Maximum ( $\text{VPD}_{\max}$ ) and mean ( $\text{VPD}_{\text{mean}}$ ) daily VPD were generated for each sampling day.

## 2.3 | Vegetation quality, topography and distance from buffer-oil-palm edge

To understand how vegetation quality and topography influence microclimate in riparian habitats we used airborne LiDAR data collected over part of the landscape (see Jucker et al., 2018). For the 35 transects coinciding with the 2014 LiDAR information, we extracted a set of vegetation and topographic metrics from the canopy height, digital terrain and plant area index model rasters, using a 12.5-m radius extraction. LiDAR-derived metrics were mean plant area index (PAI, log-transformed), maximum canopy height ( $H_{\max}$ ), topographic position index (TPI), elevation, aspect and slope. PAI was calculated empirically from the raw LiDAR data as an integrated measure of canopy density ( $\text{m}^2/\text{m}^2$ ; Holst et al., 2004).  $H_{\max}$  (m) was calculated as the maximum canopy height value (after ground-normalising the LiDAR point cloud) within 12.5 m of the logger. Four topographic covariates were calculated using the *terrain* function in the RASTER package (Hijmans, 2016) in R 3.6.1 (R Development Core Team, 2008): elevation (in m a.s.l.), slope (in degrees), aspect (in radians) and TPI—the difference between the elevation of a point and the average of its surroundings (positive values on ridges and negative values in depressions). Aspect was sinewave transformed so that east- and west-facing slopes had positive and negative values respectively. Our metrics were selected a priori following Jucker et al. (2018), who chose them due to their weak correlation (see Figure S1), and known effects on microclimate in tropical rainforests. The distance into riparian buffers from the buffer-oil-palm edge was measured on the canopy height model in QGIS 3.10.4 using the ruler tool (QGIS Development Team, 2020), as a proxy for examining the

effects of manipulating buffer width on microclimate. For dataloggers associated with riparian buffers outside the LiDAR area ( $n = 22$  transects), distances from the buffer-oil-palm edge were measured manually for buffer edge sites. River width was subtracted from total buffer width (as calculated from Google Earth imagery) and halved to give an estimate of buffer width for each transect. Distance from river was then subtracted from buffer width to give estimates of distance from edge for buffer core sites.

## 2.4 | Dung beetle diversity sampling

To understand how microclimate impacts the efficacy of riparian buffers as a means of supporting biodiversity, we carried out two dung beetle (*Scarabaeinae*) sampling campaigns, in January 2015 and from September 2017 to March 2018. The climate in our study landscape is relatively aseasonal (Walsh & Newbery, 1999), although sampling dates broadly correspond to the marginally wetter season (Marsh & Greer, 1992), where dung beetle activity is highest. Dung beetles are a useful indicator group due to their sensitivity to disturbance, high diversity, well-established taxonomy, ease of sampling and importance for a range of ecosystem functions (Nichols & Gardner, 2013). Like most tropical ectotherms, dung beetles are thought to be operating close to their thermal maxima, putting them at a greater risk of extinction due to climatic shifts (Deutsch et al., 2008). Dung beetle assemblages were sampled using human-dung-baited pitfall traps (following Slade et al., 2011). For each datalogger transect in a buffer ( $n = 48$ ), one trap was deployed for two trapping nights ~10 m from the river. The minimum distance between transects with traps was 381 m. Beetles were collected into 90% ethanol and identified to species or morpho-species using reference collections housed at the Universiti Malaysia Sabah.

## 2.5 | Statistical analyses

### 2.5.1 | Riparian buffers as microclimatic refugia

To examine whether riparian buffers and plantations maintain microclimatic conditions similar to those found in continuous riparian forest, we ran a mixed-effects model of each of our four microclimatic response variables ( $T_{\max}$ ,  $T_{\text{mean}}$ ,  $VPD_{\max}$  and  $VPD_{\text{mean}}$ ) against a fixed effect of four habitat types: continuous forest, riparian buffer core (buffer interior > 10 m from the buffer-oil-palm edge, hereafter referred to as buffer core), riparian buffer edge (buffer interior  $\leq$  10 m of the buffer-oil-palm edge, hereafter referred to as buffer edge) and oil palm. Sampling transect was fitted as a random effect, and models were run in the lme4 package in R (Bates et al., 2015) with a Gaussian error distribution. Habitat-type models were compared against the null model (only containing the random-effect) by comparing AIC, where a difference of  $-4$  supports one nested model over another (Bolker, 2008).

### 2.5.2 | Effects of vegetation quality and topography on microclimate

To analyse the effects of vegetation quality and topography on microclimate, we took a subset of our data from 36 transects that coincided with LiDAR information. We defined separate maximal linear mixed-effects models for each of our four microclimatic response variables ( $T_{\max}$ ,  $T_{\text{mean}}$ ,  $VPD_{\max}$  and  $VPD_{\text{mean}}$ ) with all of our seven explanatory variables (PAI,  $H_{\max}$ , TPI, elevation, aspect, slope and habitat) fitted as fixed effects, and with one interaction term ( $H_{\max}$ : aspect) following Jucker et al. (2018), with sampling transect as a random effect and a Gaussian error distribution. By sequential removal of terms, every possible subset of each maximal model was generated (159 for each response variable) and ranked by AIC weight in the BBMLE package in R (Bolker & R Development Core Team, 2017). Models were then subsetted to retain the fewest possible models that cumulatively accounted for 0.95 or more of the total AIC weight. The AIC weighted proportion of explanatory variable retention in the final models is reported.

### 2.5.3 | Edge effects on buffer microclimate

We examined the impact of edge effects on microclimatic conditions using distance from buffer-oil-palm edge. We analysed a subset of the full data that only included dataloggers deployed within riparian buffers (both buffer edge and core habitat types). Similar to the aforementioned habitat type analyses, each of the four microclimatic response variables ( $T_{\max}$ ,  $T_{\text{mean}}$ ,  $VPD_{\max}$  and  $VPD_{\text{mean}}$ ) were entered into mixed-effects models with distance into buffer from edge fitted as a fixed effect, sampling transect as a random effect and a Gaussian error distribution. Models were then compared to respective null models using AIC.

### 2.5.4 | Buffer microclimate impacts on dung beetle diversity

To analyse how riparian buffer microclimate impacts biodiversity, we matched our dung beetle assemblage samples to buffer core dataloggers. Microclimate data from sites 5 m from the river were used, unless data were only available from points 15 m from the river. Dung beetle diversity, calculated as Shannon diversity in the VEGAN package in R (Oksanen et al., 2010), was fitted as the response variable in four maximal linear models (for each of  $T_{\max}$ ,  $T_{\text{mean}}$ ,  $VPD_{\max}$  and  $VPD_{\text{mean}}$ ) with a Gaussian error distribution. Each maximal model had distance from buffer edge (log-transformed), the microclimate variable of interest and an interaction term between the two, as explanatory variables. For each microclimatic explanatory variable, all possible combinations of explanatory variables were compared to the maximal model using  $dAIC$ . Similar analyses were conducted for species richness (see Appendix S1).

### 3 | RESULTS

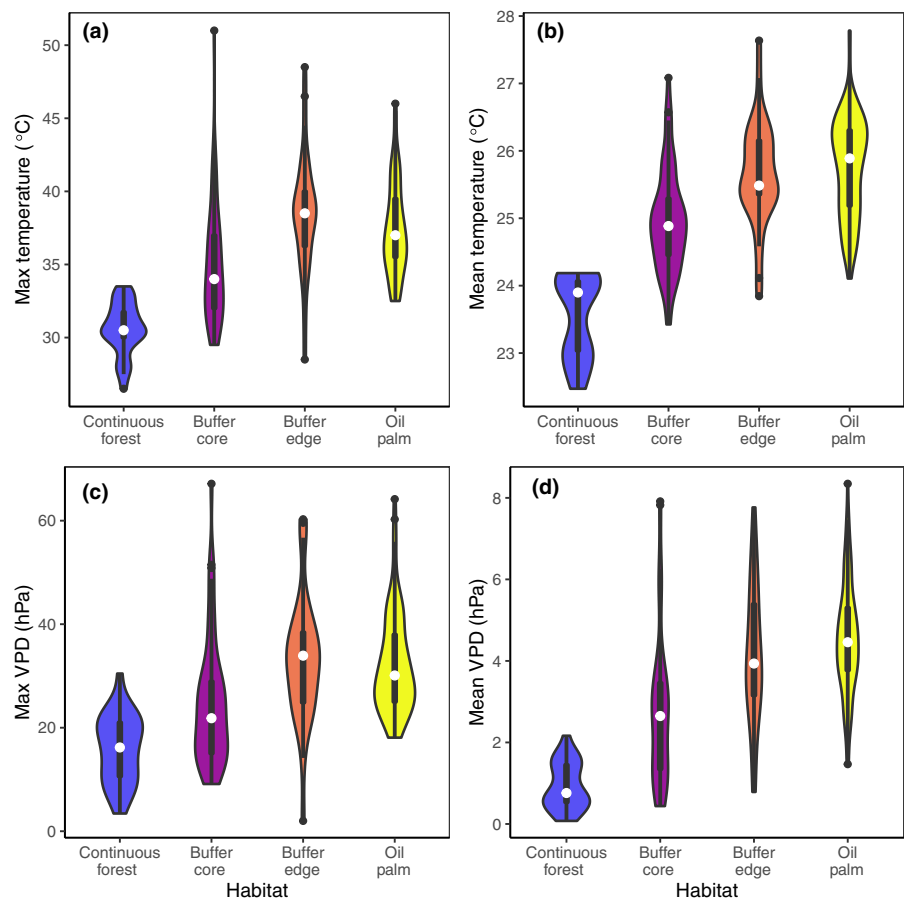
Of the 300 dataloggers deployed in riparian transects, 198 were recovered fully functioning, resulting in 5,438 days of microclimatic recordings. Of the 198 units, 110 were recovered within the LiDAR area, while 79 were located in riparian buffer core or edge and had width data available (see Table S1). All microclimatic variables ( $T_{\max}$ ,  $T_{\text{mean}}$ ,  $\text{VPD}_{\max}$  and  $\text{VPD}_{\text{mean}}$ ) were strongly correlated (Pearson's  $r > 0.6$ , see Table S2).

#### 3.1 | Riparian buffers as microclimatic refugia

We found strong support for the impact of habitat type on  $T_{\max}$ ,  $T_{\text{mean}}$ ,  $\text{VPD}_{\max}$  and  $\text{VPD}_{\text{mean}}$ , when compared to a null model (fitted with only a random effect of transect; dAICs:  $T_{\max} = -53.5$ ;  $T_{\text{mean}} = -100.9$ ;  $\text{VPD}_{\max} = -40.8$ ;  $\text{VPD}_{\text{mean}} = -91.6$ ). All microclimatic variables showed similar responses to habitat type (Figure 2), with the coolest and wettest conditions in continuous riparian forest (Table 1). Buffer core microclimates were intermediate between continuous forest and the hotter and drier oil palm, whereas buffer edge sites had maximum daily values greater than those of oil palm, and mean daily values similar to, or slightly less than, those of oil palm (Table 1).

#### 3.2 | Effects of vegetation quality and topography on microclimate

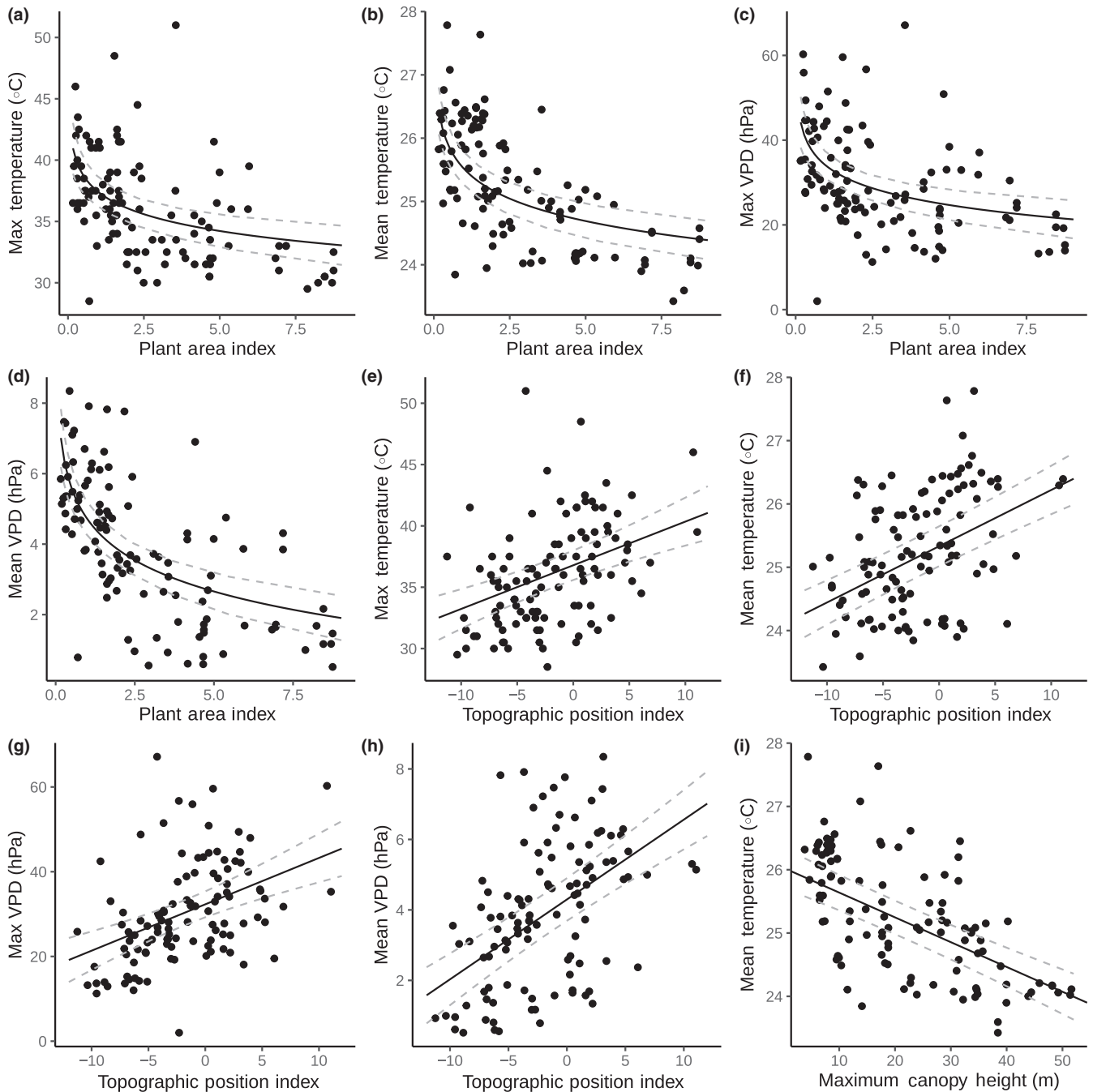
Data from units within the LiDAR area were used to model the impacts of vegetation quality and topography on microclimate across the study landscape, encompassing the riparian buffers and other habitat types. Of the best-fitting models that cumulatively accounted for an AIC weight of 0.95, the lowest-weighted models were still strongly supported when compared to the null model for each microclimatic variable (dAIC:  $T_{\max} = -45.89$ ;  $T_{\text{mean}} = -113.05$ ;  $\text{VPD}_{\max} = -21.21$ ;  $\text{VPD}_{\text{mean}} = -72.29$ ). In these best-fitting models, variables relating to both vegetation quality and topography were retained. Specifically, PAI was a strong negative predictor of all four microclimatic variables and  $H_{\max}$  was a negative predictor of  $T_{\text{mean}}$  (Figure 3; Table 2). TPI was a strong positive predictor of all four microclimatic variables (Figure 3). Elevation was a weak predictor of  $T_{\max}$  and  $T_{\text{mean}}$ , with an increase of 100 m elevation resulting in a mean drop of 0.27°C (Table 2). Aspect was a weak predictor of  $T_{\text{mean}}$  and  $\text{VPD}_{\text{mean}}$ , with east-facing slopes being hotter and drier than west-facing slopes (Table 2). Slope and the interaction term between  $H_{\max}$  and aspect were not frequently retained in best-fitting models (Table 2). Habitat type, the only non-LiDAR derived variable, was retained in the best-fitting models for  $T_{\max}$ ,  $T_{\text{mean}}$  and  $\text{VPD}_{\text{mean}}$  (Table 2).



**FIGURE 2** Violin plots of daily maximum ( $T_{\max}$ , panel a), and mean ( $T_{\text{mean}}$ , panel b) temperature, and daily maximum ( $\text{VPD}_{\max}$ , panel c) and mean ( $\text{VPD}_{\text{mean}}$ , panel d) vapour pressure deficit across habitat types. White circles are median values, the boxes are between the hinge values (25th and 75th percentiles), and the whiskers are the hinge values + or - interquartile range \* 1.5. Data that lie outside of the box and whisker plots are denoted by dark circles

**TABLE 1** Effect sizes and standard errors of habitat type on  $T_{\max}$ ,  $T_{\text{mean}}$ ,  $\text{VPD}_{\max}$  and  $\text{VPD}_{\text{mean}}$  using linear mixed-effects models

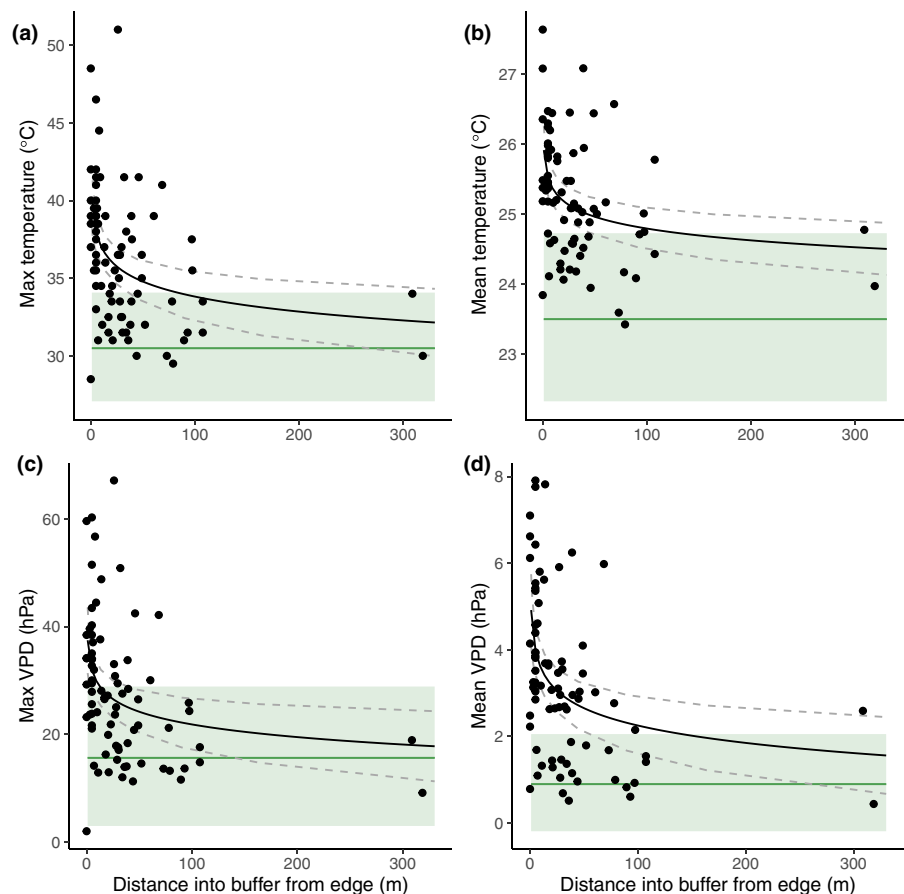
Response variables	Continuous forest		Riparian buffer		Buffer edge		Oil palm	
	Estimate	SE	Estimate	SE	Estimate	SE	Estimate	SE
$T_{\max}$ ( $^{\circ}\text{C}$ )	30.57	0.34	35.05	0.58	38.45	0.73	37.37	0.33
$T_{\text{mean}}$ ( $^{\circ}\text{C}$ )	23.53	0.12	24.96	0.11	25.66	0.14	25.75	0.08
$\text{VPD}_{\max}$ (hPa)	15.92	1.27	24.76	1.71	33.08	2.20	32.20	1.01
$\text{VPD}_{\text{mean}}$ (hPa)	0.93	0.11	2.71	0.25	4.15	0.31	4.53	0.14

**FIGURE 3** Scatter plots showing the effect of Plant Area Index (PAI; a–d) and Topographic Position Index (TPI; e–h) on  $T_{\max}$ ,  $T_{\text{mean}}$ ,  $\text{VPD}_{\max}$  and  $\text{VPD}_{\text{mean}}$ , and the effect of maximum canopy height ( $H_{\max}$ ) on  $T_{\text{mean}}$  (i). Solid lines are estimated effects from linear mixed-effects models where TPI or PAI were the only fixed effect, with dashed lines denoting 95% confidence intervals. PAI is back-transformed from data used in analyses. A positive TPI is associated with ridges and a negative TPI with depressions

**TABLE 2** Weighted proportions of the retention of each fixed effect across best-fitting models for  $T_{\max}$ ,  $T_{\text{mean}}$ ,  $\text{VPD}_{\max}$  and  $\text{VPD}_{\text{mean}}$ . AIC weights were generated for all models, before models were subsetting to include only those that cumulatively made up 0.95 of the total weight. AIC w. prop. is the proportion of the 0.95 cumulative weight constituted by models containing the fixed effect of interest. Values given in bold fell above an arbitrary threshold value of 0.5. Effect sizes of models with only a single explanatory variable are given, with the exception of habitat, as it is a categorical variable (see Table 1). PAI, TPI and  $H_{\max}$  are abbreviations for Plant Area Index, Topographic Position Index and maximum canopy height respectively. A positive TPI is associated with ridges and a negative TPI with depressions

Fixed effects	$T_{\max}$		$T_{\text{mean}}$		$\text{VPD}_{\max}$		$\text{VPD}_{\text{mean}}$	
	AIC w. prop.	Effect	AIC w. prop.	Effect	AIC w. prop.	Effect	AIC w. prop.	Effect
PAI	<b>0.930</b>	<b>-1.980</b>	<b>1.000</b>	<b>-0.512</b>	<b>0.950</b>	<b>-5.726</b>	<b>1.000</b>	<b>-1.279</b>
$H_{\max}$	0.362	-0.134	<b>0.642</b>	<b>-0.039</b>	0.324	-0.384	0.410	-0.095
TPI	<b>0.899</b>	<b>0.357</b>	<b>1.000</b>	<b>0.089</b>	<b>0.924</b>	<b>1.096</b>	<b>0.955</b>	<b>0.226</b>
Elevation	<b>0.692</b>	<b>-0.0011</b>	<b>1.000</b>	<b>-0.0027</b>	0.275	-0.0010	0.273	0.0048
Aspect	0.366	0.182	<b>0.978</b>	<b>0.224</b>	0.304	1.640	<b>0.559</b>	<b>0.427</b>
Slope	0.310	-3.024	0.463	-1.58	0.273	-9.229	0.258	-4.041
Aspect: $H_{\max}$	0.090	0.220	0.176	0.072	0.047	0.006	0.065	0.011
Habitat type	<b>1.000</b>	—	<b>1.000</b>	—	0.467	—	<b>0.861</b>	—

**FIGURE 4** Scatter plots showing the effect of distance into the buffer from the buffer-oil-palm edge on  $T_{\max}$ ,  $T_{\text{mean}}$ ,  $\text{VPD}_{\max}$  and  $\text{VPD}_{\text{mean}}$  (panels a, b c and d, respectively). Black lines are back-transformed from log-transformed distance predicted from linear mixed effects models, with dashed lines denoting 95% confidence intervals. Solid green lines denote mean microclimatic values for continuous riparian forest, with 95% confidence intervals shown in green bands



### 3.3 | Edge effects on buffer microclimate

Linear mixed-effects models of distance into the buffer from the buffer-oil-palm edge (log-transformed) were strongly supported when compared to the null models (dAIC:  $T_{\max} = -15.65$ ;  $T_{\text{mean}} = -20.75$ ;  $\text{VPD}_{\max} = -10.58$ ;  $\text{VPD}_{\text{mean}} = -17.96$ ). All microclimatic response variables had negative relationships with

distance from edge ( $T_{\max} = -1.40 \pm 0.31$ ,  $T_{\text{mean}} = -0.24 \pm 0.05$ ,  $\text{VPD}_{\max} = -3.39 \pm 0.93$ ,  $\text{VPD}_{\text{mean}} = -0.58 \pm 0.12$ ; Figure 4). At approximately 80–120 m from the edge, predicted curves for each microclimatic variable become relatively flat, and for  $T_{\max}$ ,  $T_{\text{mean}}$  and  $\text{VPD}_{\text{mean}}$  begin to be comparable to those of continuous riparian forest values, (Figure 4). All models had Cook's distances < 0.5 (see Figure S2).

### 3.4 | Buffer microclimate impacts on dung beetle diversity

Of the 48 transects associated with riparian buffers, 31 had functioning dataloggers in the buffer core, with associated data on both dung beetle diversity and distance from edge into buffer. Dung beetle diversity was driven by an interaction between distance from buffer edge and both  $T_{\max}$  and  $T_{\text{mean}}$  (Table 3). As distance from the edge decreased, the relationship between temperature ( $T_{\max}$  and  $T_{\text{mean}}$ ) and dung beetle diversity became more negative, whereas at 80 m it is relatively flat (Figure 5). Responses for the interaction between VPD and distance from edge were similar to those of temperature but with lower AIC weight, particularly for  $\text{VPD}_{\text{mean}}$  (Table 3). Further, lower dung beetle diversity was associated with higher  $T_{\text{mean}}$ ,  $\text{VPD}_{\max}$  and  $\text{VPD}_{\text{mean}}$  (Tables 3 and 4). Note, the  $\text{VPD}_{\max}$  model lacking an interaction term failed our leverage tests and must be regarded with caution (see Figure S3). Species richness analyses showed similar responses to Shannon diversity (see Appendix S1).

**TABLE 3** AIC weights of all models of Shannon Diversity for each microclimatic variable ( $T_{\max}$ ,  $T_{\text{mean}}$ ,  $\text{VPD}_{\max}$  and  $\text{VPD}_{\text{mean}}$ ), where 'interaction' denotes models containing the interaction term between buffer width and microclimate, 'additive' denotes a model containing microclimate and buffer width, 'buffer width' and 'microclimate' denote models containing only that term, and 'null' is the null model. Values given in bold make up the best-fitting models, as calculated by a cumulative ranked weight  $>0.95$

Models	$T_{\max}$	$T_{\text{mean}}$	$\text{VPD}_{\max}$	$\text{VPD}_{\text{mean}}$
Interaction	<b>0.959</b>	<b>0.914</b>	<b>0.723</b>	<b>0.354</b>
Additive	0.038	<b>0.068</b>	<b>0.271</b>	<b>0.573</b>
Buffer width	0.003	0.018	0.005	<b>0.068</b>
Microclimate	$<0.001$	$<0.001$	$<0.001$	0.005
Null	$<0.001$	$<0.001$	$<0.001$	0.001

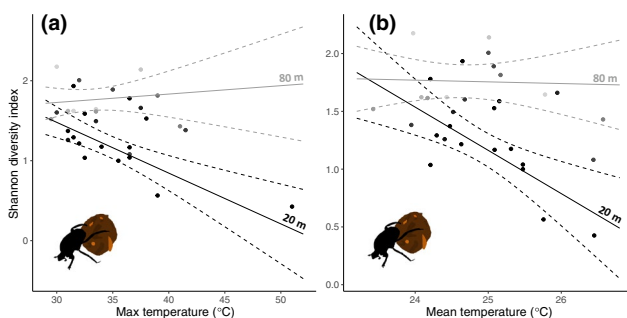


**FIGURE 5** Visualisations of the interaction between the effects of (a)  $T_{\max}$  and (b)  $T_{\text{mean}}$ , and distance from edge on dung beetle diversity. Solid lines give the effect of temperature on diversity, given two set distances (20 and 80 m) from the edge of the buffer, as predicted using estimates from linear models (see Table 3), with dashed lines denoting 95% confidence intervals. Grey-scaling on points and lines gives the magnitude of distance from buffer edge (grey  $>$  black)

**TABLE 4** Outputs of best-fitting linear models predicting the Shannon diversity of dung beetles ( $H'$ ) sampled in riparian buffers. In the model column '~' means 'as a function of' and '\*' means the two terms individually and the interaction between the two are included

Model	Term	Estimate	SE
$H' \sim T_{\max} * \text{distance from edge}$	Intercept	7.645	2.215
	$T_{\max}$	-0.223	0.067
	Distance from edge	-1.422	0.607
	$T_{\max} : \text{distance from edge}$	0.053	0.018
$H' \sim T_{\max} + \text{distance from edge}$	Intercept	1.355	0.532
	$T_{\max}$	-0.032	0.012
	Distance from edge	0.333	0.073
$H' \sim T_{\text{mean}} * \text{distance from edge}$	Intercept	28.66	9.446
	$T_{\text{mean}}$	-1.151	0.382
	Distance from edge	-6.057	2.407
	$T_{\text{mean}} : \text{distance from edge}$	0.259	0.098
$H' \sim T_{\text{mean}} + \text{distance from edge}$	Intercept	3.939	1.821
	$T_{\text{mean}}$	-0.150	0.070
	Distance from edge	0.338	0.077
$H' \sim \text{VPD}_{\max} * \text{distance from edge}$	Intercept	1.398	0.485
	$\text{VPD}_{\max}$	-0.053	0.021
	Distance from edge	0.903	0.129
	$\text{VPD}_{\max} : \text{distance from edge}$	0.012	0.006
$H' \sim \text{VPD}_{\max} + \text{distance from edge}$	Intercept	0.668	0.315
	$\text{VPD}_{\max}$	-0.013	0.004
	Distance from edge	0.300	0.072
$H' \sim \text{VPD}_{\text{mean}} * \text{distance from edge}$	Intercept	0.869	0.434
	$\text{VPD}_{\text{mean}}$	-0.216	0.142
	Distance from edge	0.214	0.109
	$\text{VPD}_{\text{mean}} : \text{distance from edge}$	0.039	0.041
$H' \sim \text{VPD}_{\text{mean}} + \text{distance from edge}$	Intercept	0.617	0.345
	$\text{VPD}_{\text{mean}}$	-0.084	0.033
	Distance from edge	0.285	0.080
$H' \sim \text{distance from edge}$	Intercept	0.104	0.302
	Distance from edge	0.365	0.080

## 4 | DISCUSSION

Our results demonstrate the capacity of riparian buffers to provide microclimatic refugia in human-modified tropical landscapes. All four measures of temperature and vapour pressure deficit ( $T_{\max}$ ,  $T_{\text{mean}}$ ,  $\text{VPD}_{\max}$  and  $\text{VPD}_{\text{mean}}$ ) were lower in the core area of riparian buffers than in the surrounding oil palm, although these values were

still higher than those in continuous riparian forest. We reveal that buffer edge effects mediate microclimate, with the interior of the buffer being substantially cooler and more humid than edges and plantation. We subsequently demonstrate the key roles that greater vegetation complexity and topographic sheltering play in increasing the microclimatic buffering capacity of these set-asides. Finally, we elucidate the link between buffer width and microclimate, and dung beetle communities, revealing that proximity-to-edge and temperature can synergistically decrease local diversity.

Consistent with our results, Nagy et al. (2015) found that microclimates in riparian buffer cores in the southern Amazon were comparable to those of continuous riparian forests. Cooler and wetter conditions here were more strongly associated with wide buffers, particularly those 80 m or more in width (Table 5). Although our buffer core sites were generally cooler than oil palm, edge habitat was characterised by more extreme conditions than adjacent plantation. Oil palm is a perennial crop with a peak yield occurring at an age of 9–18 years (Alam et al., 2015), with older plantations forming tall canopies with cooler microclimates (Luskin & Potts, 2011). We postulate that high  $T_{\max}$  and  $VPD_{\max}$  in buffer edges is due to gaps in vegetation associated with riparian buffer edges (JW personal observation). Such gaps are dominated by bare ground, grasses or low-lying vines, and may be due to clearing and spillover of herbicides from the plantation. The gaps could also elevate  $T$  and  $VPD$  for short periods of the day. The temperature and humidity extremes in buffer edges are consistent with well-documented microclimatic changes seen in other edge habitats, which are typically attributed to increased solar radiation and wind (see Williams-Linera, 1990).

We reveal the link between several vegetation and topographic features, and microclimate, across a human-modified tropical landscape. In particular, PAI, a measure of vegetation quality, had a strong influence on microclimate. Increased PAI is associated with more complex vegetation (Holst et al., 2004), causing decreased wind and light exposure to give cool, humid conditions (Hardwick et al., 2015).  $H_{\max}$  (maximum canopy height) was also strongly associated with  $T_{\max}$ , a relationship driven by increased shading by tall trees (Jucker et al., 2018). Like other edge habitats, riparian buffers are characterised by factors impacting vegetation structure, with reduced seedling abundance, tree basal area, canopy height and woody plant diversity compared with continuous riparian forest (Keir et al., 2015; Lees & Peres, 2007; Nagy et al., 2015). Topography was also a key predictor of our microclimatic variables, with TPI having strong positive correlations with temperature and  $VPD$ . Such results are indicative of the relative exposure of ridges (high TPI) and depressions (low TPI) to

light and wind (Dobrowski, 2011). Aspect had a small positive effect on  $T_{\max}$  and  $VPD_{\max}$ , where east-facing slopes tended to be hotter and drier, likely due to daily solar radiation and wind patterns in the region (Smith, 1977). Elevation negatively predicted  $T_{\max}$  and  $T_{\max}$ , with a 100-m increase resulting in a mean drop of 0.27°C, a lower impact than we might expect given the literature (Jucker et al., 2018) and likely due to a limited range of elevations in our study. Our results highlight the importance of understanding how heterogeneous vegetation and topography must be taken into account when defining the extent of riparian buffers in environmental policies, as well as predicting landscape- or regional-level diversity responses under climate change scenarios (Elsen et al., 2020).

The cooler, wetter microclimate of riparian buffers described here makes them likely refugia for biodiversity in a hostile agricultural matrix. Indeed, our results indicate that microclimate in buffers may be important for driving diversity patterns in dung beetles, a key invertebrate indicator group. We found that at 80 m from the edge, the response of beetle diversity to temperature was negligible. However, as proximity to the buffer-oil-palm edge increased, the negative effects of temperature on diversity were amplified, with beetle communities in 20 m buffers acutely sensitive to higher temperatures. Previous research within the same landscape found riparian buffers support higher diversity than surrounding oil palm plantations, with dung beetle assemblages more similar to those of continuous riparian forests than oil palm (Gray et al., 2014). Further, Gray et al. (2016) demonstrated little spillover of dung beetle species within riparian buffers into the surrounding oil palm plantations. Combined with our findings, this suggests that riparian buffers may act as microrefugia for forest invertebrates. Note that the effects of microclimatic variables shown here could be correlative rather than causative. As we have demonstrated, topography and vegetation complexity can also drive microclimatic conditions, and it is difficult to disentangle these effects. This does not however, change the take-home message of the results—to maximise co-benefits for terrestrial biodiversity in riparian buffers, simply regulating buffer width alone is likely to be insufficient if this does not preserve the vegetation and topographic features that are needed to help maintain a buffered microclimate.

In addition to microclimate, we also found that distance from edge was associated with higher local diversity, supporting a pool of literature demonstrating the positive impact of increased buffer width on terrestrial biodiversity (Gray et al., 2017; Keir et al., 2015; Zimbres et al., 2018). Intriguingly, the widths recommended by these previous studies to retain terrestrial biodiversity

**TABLE 5** Microclimate buffering with distance inward from buffer edge, as estimated from linear mixed-effects models. Values given reflect the difference relative to the microclimate in oil palm (Table 1)

Response variables	5 m	20 m	40 m	80 m	300 m
$T_{\max}$ (°C)	0.36	-1.58	-2.55	-3.51	-5.36
$T_{\text{mean}}$ (°C)	-0.23	-0.57	-0.73	-0.90	-1.23
$VPD_{\max}$ (hPa)	-0.80	-5.50	-7.85	-10.21	-14.69
$VPD_{\text{mean}}$ (hPa)	-0.57	-1.37	-1.77	-2.17	-2.94

(80 m for dung beetles and forest-specialising birds; Gray et al., 2017; Mitchell et al., 2018) are in the region where some of our proximity-to-edge microclimatic response curves intersect with the 95% confidence interval for continuous forest and where edge effects generally tail off in many systems (e.g. Didham & Lawton, 1999; Laurance et al., 2002). The consequences of edge effects for biodiversity may be more pronounced in tropical landscapes with sparse open habitat where species have not experienced long-term selection pressures for avoiding edges (Betts et al., 2020). Ideally, edge effects would be investigated in the same set of models as vegetation quality; however, due to strong correlations between proximity-to-edge and our LiDAR-derived variables, this was not possible.

#### 4.1 | Policy implications

Our results are important to riparian buffer policies in human-modified tropical landscapes, supporting suggestions that mandatory riparian buffer widths in the tropics should be wider than they currently are, that more attention should be given to buffer habitat quality (Luke, Slade, et al., 2019), and that topography should also be considered when planning networks of buffers across landscapes. We show that buffers begin to reach microclimatic conditions comparable to those of continuous riparian forest at approximately 80 m and above, on each side of the river, a width previously suggested as adequate for maintaining representative levels of species diversity (Gray et al., 2017; Mitchell et al., 2018). At this buffer width, the negative impacts of temperature on biodiversity are far less pronounced than at 20 m, the width typically required by law in Sabah, Malaysia. These recommendations are emphasised by the finding that buffer edges, and thus narrow buffers (<10 m), may be more microclimatically extreme than no buffer at all. In addition, many tropical countries do not consider vegetation complexity in riparian management policies (Luke, Slade, et al., 2019), but doing so could help contribute to improved microclimate conditions and long-term sustainability of waterways in agricultural areas. We therefore advocate efforts to extend buffer widths, prevent further degradation and restore riparian buffers (Luke, Advento, et al., 2019). In addition, by determining the vegetation and topographic features that drive microclimate in tropical riparian buffers, we hope to inform the future planning of buffer locations and networks. Taken together, our results suggest that safeguarding riparian buffer microclimate may help to limit the local extinction of species by providing microrefugia. This finding is likely to become increasingly important in the face of anthropogenic climate change (Hampe & Jump, 2011), particularly if demand for agricultural land near waterbodies increases with drier climates.

#### ACKNOWLEDGEMENTS

This work was funded by the Natural Environmental Research Council (NERC) through the Human Modified Tropical Forests programme (NE/K016261/1; NE/K016377/1), as well as the

Newton-Ungku Omar Fund via the British Council and Malaysian Industry Government Group for High Technology (216433953). NERC also funded the PhD studentship for J.W. (NE/L002485/1) and research fellowship of T.J. (NE/S01537X/1). We are grateful to the Sabah Biodiversity Council for permission to conduct the fieldwork (S.H.L.: JKM/MBS.1000-2/2JLD.5(13); J.W.: JKM/MBS.1000-2/2JLD.7(83); E.M.S.: JKM/MBS.1000-2/2(381)), Jonathan Parrett for help with dung beetle identification, Sui Peng Heon for translating the abstract into Malay, Matilda Brindle for proof-reading the manuscript and the South East Asian Rainforest Research Programme staff, who made this work possible: Unding Jami, Johnny Larenus, Amir, Anis, David, Didy, Dino, Joanni, Kiki, Loly, Mudin, Noy and Zul.

#### AUTHORS' CONTRIBUTIONS

M.J.S. and E.M.S. conceived the initial project and research design; S.H.L., E.M.S. and H.H. undertook the fieldwork; T.S., T.J. and D.A.C. contributed LiDAR data; J.W. and E.M.S. identified the dung beetles with support from AYCC; J.W. led the analysis and writing of the manuscript with input from the rest of the team.

#### DATA AVAILABILITY STATEMENT

Microclimate data available via <https://doi.org/10.5281/zenodo.4000206> (Williamson et al., 2020). LiDAR data available via <https://doi.org/10.5281/zenodo.4020697> (Swinfield et al., 2020). Dung beetle data for 2015 and 2017/2018 available via <https://doi.org/10.5281/zenodo.3906118> and <https://doi.org/10.5281/zenodo.3906441> (Slade, Milne, et al., 2020; Slade, Williamson, et al., 2020).

#### ORCID

Joseph Williamson  <https://orcid.org/0000-0003-4916-5386>  
 Eleanor M. Slade  <https://orcid.org/0000-0002-6108-1196>  
 Sarah H. Luke  <https://orcid.org/0000-0002-8335-5960>  
 Tom Swinfield  <https://orcid.org/0000-0001-9354-5090>  
 Arthur Y. C. Chung  <https://orcid.org/0000-0002-9529-4114>  
 David A. Coomes  <https://orcid.org/0000-0002-8261-2582>  
 Tommaso Jucker  <https://orcid.org/0000-0002-0751-6312>  
 Owen T. Lewis  <https://orcid.org/0000-0001-7935-6111>  
 Charles S. Vairappan  <https://orcid.org/0000-0001-7453-1718>  
 Stephen J. Rossiter  <https://orcid.org/0000-0002-3881-4515>  
 Matthew J. Struebig  <https://orcid.org/0000-0003-2058-8502>

#### REFERENCES

- Alam, A. F., Er, A. C., & Begum, H. (2015). Malaysian oil palm industry: Prospect and problem. *Journal of Food, Agriculture & Environment*, 13(2), 143–148.
- Allan, J. D. (2004). Landscapes and riverscapes: The influence of land use on stream ecosystems. *Annual Review of Ecology, Evolution and Systematics*, 35, 257–284. <https://doi.org/10.1146/annurev.ecolsys.35.120202.110122>
- Barlow, J., Louzada, J., Parry, L., Hernández, M. I. M., Hawes, J., Peres, C. A., Vaz-de-Mello, F. Z., & Gardner, T. A. (2010). Improving the design and management of forest strips in human-dominated tropical landscapes: A field test on Amazonian dung beetles. *Journal of Applied Ecology*, 47, 779–788. <https://doi.org/10.1111/j.1365-2664.2010.01825.x>

- Bates, D., Maechler, M., Bolker, B., & Walker, S. (2015). Fitting linear mixed-effects models using lme4. *Journal of Statistical Software*, 67(1), 1–48.
- Betts, M. G., Wolf, C., Pfeifer, M., Banks-Leite, C., Arroyo-Rodríguez, V., Ribeiro, D. B., Barlow, J., Eigenbrod, F., Faria, D., Fletcher, R. J., Hadley, A. S., Hawes, J. E., Holt, R. D., Klingbeil, B., Kormann, U., Lens, L., Levi, T., Medina-Rangel, G. F., Melles, S. L., ... Ewers, R. M. (2020). Extinction filters mediate the global effects of habitat fragmentation on animals. *Science*, 366(6470), 1236–1239. <https://doi.org/10.1126/science.aax9387>
- Blonder, B., Both, S., Coomes, D. A., Elias, D., Jucker, T., Kvasnica, J., Majalap, N., Malhi, Y. S., Milodowski, D., Riutta, T., & Svátek, M. (2018). Extreme and highly heterogeneous microclimates in selectively logged tropical forests. *Frontiers in Forests and Global Change*, 1, 5. <https://doi.org/10.3389/ffgc.2018.00005>
- Bolker, B. M. (2008). *Ecological models and data in R* (p. 210). Princeton University Press.
- Bolker, B. & R Development Core Team. (2017). *bbmle: Tools for general maximum likelihood estimation*. R package version 1.0.20. Retrieved from <https://cran.r-project.org/web/packages/bbmle/index.html>
- Chapman, S., Syktus, J., Trancoso, R., Salazar, A., Thatcher, M., Watson, J. E. M., Meijaard, E., Sheil, D., Dargusch, P., & McAlpine, C. A. (2020). Compounding impact of deforestation on Borneo's climate during El Niño events. *Environmental Research Letters*, 15, 084006. <https://doi.org/10.1088/1748-9326/AB86F5>
- Cunha, E. J., & Juen, L. (2017). Impacts of oil palm plantations on changes in environmental heterogeneity and Heteroptera (Gerromorpha and Nepomorpha) diversity. *Journal of Insect Conservation*, 21, 111–119. <https://doi.org/10.1007/s10841-017-9959-1>
- Deutsch, C. A., Tewksbury, J. J., Huey, R. B., Sheldon, K. S., Ghalambor, C. K., Haak, D. C., & Martin, P. R. (2008). Impacts of climate warming on terrestrial ectotherms across latitude. *Proceedings of the National Academy of Sciences of the United States of America*, 105(18), 6668–6672. <https://doi.org/10.1073/pnas.0709472105>
- Didham, R. K., & Lawton, J. H. (1999). Edge structure determines the magnitude of changes in microclimate and vegetation structure in tropical forest fragments. *Biotropica*, 31(1), 17–30. <https://doi.org/10.1111/j.1744-7429.1999.tb00113.x>
- Dobrowski, S. Z. (2011). A climatic basis for microrefugia: The influence of terrain on climate. *Global Change Biology*, 17(2), 1022–1035. <https://doi.org/10.1111/j.1365-2486.2010.02263.x>
- Elsen, P. R., Monahan, W. B., & Merenlender, A. M. (2020). Topography and human pressure in mountain ranges alter expected species responses to climate change. *Nature Communications*, 11(1), 1–10. <https://doi.org/10.1038/s41467-020-15881-x>
- Fick, S. E., & Hijmans, R. J. (2017). WorldClim 2: New 1-km spatial resolution climate surfaces for global land areas. *International Journal of Climatology*, 37(12), 4302–4315. <https://doi.org/10.1002/joc.5086>
- Giam, X., Hadiaty, R. K., Tan, H. H., Parenti, L. R., Wowor, D., Sauri, S., Chong, K. Y., Yeo, D. C. J., & Wilcove, D. S. (2015). Mitigating the impact of oil-palm monoculture on freshwater fishes in Southeast Asia. *Conservation Biology*, 29, 1357–1367. <https://doi.org/10.1111/cobi.12483>
- Gray, C. L., Simmons, B. I., Fayle, T. M., Mann, D. J., & Slade, E. M. (2016). Are riparian forest reserves sources of invertebrate biodiversity spillover and associated ecosystem functions in oil palm landscapes? *Biological Conservation*, 194, 176–183. <https://doi.org/10.1016/j.biocon.2015.12.017>
- Gray, C. L., Slade, E. M., Mann, D. J., & Lewis, O. T. (2014). Do riparian reserves support dung beetle biodiversity and ecosystem services in oil palm-dominated tropical landscapes? *Ecology and Evolution*, 4(7), 1049–1060. <https://doi.org/10.1002/ece3.1003>
- Gray, C., Slade, E., Mann, D., & Lewis, O. T. (2017). Designing oil palm landscapes to retain biodiversity using insights from a key ecological indicator group. *bioRxiv*. <https://doi.org/10.1101/204347>
- Gray, R. E. J., Slade, E. M., Chung, A. Y., & Lewis, O. T. (2019). Movement of moths through riparian reserves within oil palm plantations. *Frontiers in Forests and Global Change*, 2, 68. <https://doi.org/10.3389/ffgc.2019.00068>
- Hampe, A., & Jump, A. S. (2011). Climate relicts: Past, present, future. *Annual Review of Ecology, Evolution, and Systematics*, 42, 313–333. <https://doi.org/10.1146/annurev-ecolsys-102710-145015>
- Hardwick, S. R., Toumi, R., Pfeifer, M., Turner, E. C., Nilus, R., & Ewers, R. M. (2015). The relationship between leaf area index and microclimate in tropical forest and oil palm plantation: Forest disturbance drives changes in microclimate. *Agricultural and Forest Meteorology*, 201, 187–195. <https://doi.org/10.1016/j.agrformet.2014.11.010>
- Helmuth, B. (2009). From cells to coastlines: How can we use physiology to forecast the impacts of climate change? *Journal of Experimental Biology*, 212(6), 753–760. <https://doi.org/10.1242/jeb.023861>
- Hijmans, R. J. (2016). *raster: Geographic data analysis and modeling*. R package version 2.5–8. Retrieved from <https://CRAN.R-project.org/package=raster>
- Holst, T., Hauser, S., Kirchgäßner, A., Matzarakis, A., Mayer, H., & Schindler, D. (2004). Measuring and modelling plant area index in beech stands. *International Journal of Biometeorology*, 48(4), 192–201. <https://doi.org/10.1007/s00484-004-0201-y>
- Jucker, T., Hardwick, S. R., Both, S., Elias, D. M. O., Ewers, R. M., Milodowski, D. T., Swinfield, T., & Coomes, D. A. (2018). Canopy structure and topography jointly constrain the microclimate of human-modified tropical landscapes. *Global Change Biology*, 24(11), 5243–5258. <https://doi.org/10.1111/gcb.14415>
- Jucker, T., Jackson, T. D., Zellweger, F., Swinfield, T., Gregory, N., Williamson, J., Slade, E. M., Phillips, J. W., Bittencourt, P. R. L., Blonder, B., Boyle, M. J. W., Ellwood, M. D. F., Hemprich-Bennett, D., Lewis, O. T., Matula, R., Senior, R. A., Shenkin, A., Svátek, M., & Coomes, D. A. (2020). A research agenda for microclimate ecology in human-modified tropical forests. *Frontiers in Forests and Global Change*, 2, 92. <https://doi.org/10.3389/ffgc.2019.00092>
- Keir, A. F., Pearson, R. G., & Congdon, R. A. (2015). Determinants of bird assemblage composition in riparian vegetation on sugarcane farms in the Queensland wet tropics. *Pacific Conservation Biology*, 21, 60–73. <https://doi.org/10.1071/PC14904>
- Keuroghlian, A., & Eaton, D. P. (2008). Importance of rare habitats and riparian zones in a tropical forest fragment: Preferential use by *Tayassu pecari*, a wide-ranging frugivore. *Journal of Zoology*, 275(3), 283–293. <https://doi.org/10.1111/j.1469-7998.2008.00440.x>
- Laurance, W. F., Lovejoy, T. E., Vasconcelos, H. L., Bruna, E. M., Didham, R. K., Stouffer, P. C., Gascon, C., Bierregaard, R. O., Laurance, S. G., & Sampaio, E. (2002). Ecosystem decay of Amazonian forest fragments: A 22-year investigation. *Conservation Biology*, 16, 605–618. <https://doi.org/10.1046/j.1523-1739.2002.01025.x>
- Law, S. J., Bishop, T. R., Eggleton, P., Griffiths, H., Ashton, L., & Parr, C. (2020). Darker ants dominate the canopy: Testing macroecological hypotheses for patterns in colour along a microclimatic gradient. *Journal of Animal Ecology*, 89(2), 347–359. <https://doi.org/10.1111/1365-2656.13110>
- Lees, A. C., & Peres, C. A. (2008). Conservation value of remnant riparian forest corridors of varying quality for Amazonian birds and mammals. *Conservation Biology*, 22(2), 439–449. <https://doi.org/10.1111/j.1523-1739.2007.00870.x>
- Luke, S. H., Advento, A. D., Aryawan, A. A. K., Adhy, D. N., Ashton-Butt, A., Barclay, H., Dewi, J. P., Drewler, J., Dumbrell, A. J., Edi, Eycott, A. E., Harijanja, M. F., Hinsch, J. K., Hood, A. S. C., Kurniawan, C., Kurz, D. J., Mann, D. J., Matthews Nicholass, K. J., Naim, M., ... Turner, E. C. (2019). Managing oil palm plantations more sustainably: Large-scale experiments within the Biodiversity and Ecosystem Function in Tropical Agriculture (BEFTA) Programme. *Frontiers in Forests and Global Change*, 2, 75. <https://doi.org/10.3389/ffgc.2019.00075>

- Luke, S. H., Slade, E. M., Gray, C. L., Annammala, K. V., Drewer, J., Williamson, J., Agama, A. L., Ationg, M., Mitchell, S. L., Vairappan, C. S., & Struebig, M. J. (2019). Riparian buffers in tropical agriculture: Scientific support, effectiveness and directions for policy. *Journal of Applied Ecology*, 56, 85–92. <https://doi.org/10.1111/1365-2664.13280>
- Luskin, M. S., & Potts, M. D. (2011). Microclimate and habitat heterogeneity through the oil palm lifecycle. *Basic and Applied Ecology*, 12(6), 540–551. <https://doi.org/10.1016/j.baae.2011.06.004>
- Marsh, C. W., & Greer, A. G. (1992). Forest land-use in Sabah, Malaysia: An introduction to Danum Valley. *Philosophical Transactions of the Royal Society of London. Series B: Biological Sciences*, 335(1275), 331–339. <https://doi.org/10.1098/rstb.1992.0025>
- Meijide, A., Badu, C. S., Moyano, F., Tiralla, N., Gunawan, D., & Knohl, A. (2018). Impact of forest conversion to oil palm and rubber plantations on microclimate and the role of the 2015 ENSO event. *Agricultural and Forest Meteorology*, 252, 208–219. <https://doi.org/10.1016/j.agrformet.2018.01.013>
- Mitchell, S. L., Edwards, D. P., Bernard, H., Coomes, D., Jucker, T., Davies, Z. G., & Struebig, M. J. (2018). Riparian reserves help protect forest bird communities in oil palm dominated landscapes. *Journal of Applied Ecology*, 55(6), 2744–2755. <https://doi.org/10.1111/1365-2664.13233>
- Nagy, R. C., Porder, S., Neill, C., Brando, P., Quintino, R. M., & Nascimento, S. A. D. (2015). Structure and composition of altered riparian forests in an agricultural Amazonian landscape. *Ecological Applications*, 25(6), 1725–1738. <https://doi.org/10.1890/14-1740.1>
- Nichols, E. S., & Gardner, T. A. (2011). Dung beetles as a candidate study taxon in applied biodiversity conservation research. *Ecology and Evolution of Dung Beetles*, 267–291. <https://doi.org/10.1002/978144342000.ch13>
- Oksanen, J., Blanchet, F. G., Kindt, R., Legendre, P., O'hara, R. B., Simpson, G. L., & Wagner, H. (2010). *Vegan: Community ecology package*. R package version 1.17-4. Retrieved from <http://CRAN.R-project.org/package=vegan>
- Park Williams, A., Allen, C. D., Macalady, A. K., Griffin, D., Woodhouse, C. A., Meko, D. M., Swetnam, T. W., Rauscher, S. A., Seager, R., Grissino-Mayer, H. D., Dean, J. S., Cook, E. R., Gangodagamage, C., Cai, M., & McDowell, N. G. (2013). Temperature as a potent driver of regional forest drought stress and tree mortality. *Nature Climate Change*, 3(3), 292–297. <https://doi.org/10.1038/nclimate1693>
- QGIS Development Team. (2020). *QGIS geographic information system*. Open Source Geospatial Foundation Project. Retrieved from <http://qgis.osgeo.org>
- R Development Core Team. (2008). *R: A language and environment for statistical computing*. R Foundation for Statistical Computing. Retrieved from <http://www.R-project.org>. ISBN3-900051-07-0
- Schulze, C. H., Linsenmair, K. E., & Fiedler, K. (2001). Understorey versus canopy: Patterns of vertical stratification and diversity among Lepidoptera in a Bornean rain forest. *Plant Ecology*, 153, 133–152. <https://doi.org/10.1023/A:1017589711553>
- Silvério, D. V., Brando, P. M., Macedo, M. N., Beck, P. S., Bustamante, M., & Coe, M. T. (2015). Agricultural expansion dominates climate changes in southeastern Amazonia: The overlooked non-GHG forcing. *Environmental Research Letters*, 10(10), 104015. <https://doi.org/10.1088/1748-9326/10/10/104015>
- Slade, E. M., Mann, D. J., & Lewis, O. T. (2011). Biodiversity and ecosystem function of tropical forest dung beetles under contrasting logging regimes. *Biological Conservation*, 144(1), 166–174. <https://doi.org/10.1016/j.biocon.2010.08.011>
- Slade, E. M., Milne, S., Chung, A. Y. C., Williamson, J., & Parrett, J. (2020). Dung beetle community and dung removal data 2015. *Zenodo*, <https://doi.org/10.5281/zenodo.3906118>
- Slade, E. M., Williamson, J., Chung, A. Y. C., Parrett, J., & Heroín, H. (2020). Dung beetle community 2017/18. *Zenodo*, <https://doi.org/10.5281/zenodo.3906441>
- Smith, J. M. B. (1977). Vegetation and microclimate of east-and west-facing slopes in the grasslands of Mt Wilhelm, Papua New Guinea. *The Journal of Ecology*, 65(1), 39–53. <https://doi.org/10.2307/2259061>
- Struebig, M. J., Turner, A., Giles, E., Lasmana, F., Tollington, S., Bernard, H., & Bell, D. (2013). Quantifying the biodiversity value of repeatedly logged rainforests: Gradient and comparative approaches from Borneo. *Advances in Ecological Research*, 48, 183–224. <https://doi.org/10.1016/B978-0-12-417199-2.00003-3>
- Swinfield, T., Milodowski, D., Jucker, T., Dalponte, M., & Coomes, D. A. (2020). LiDAR canopy structure 2014. *Zenodo*, <https://doi.org/10.5281/zenodo.4020697>
- Tabacchi, E., Lambs, L., Guilloy, H., Planty-Tabacchi, A. M., Muller, E., & Decamps, H. (2000). Impacts of riparian vegetation on hydrological processes. *Hydrological Processes*, 14(16–17), 2959–2976. [https://doi.org/10.1002/1099-1085\(200011/12\)14:16/17<2959:AID-HYP129>3.0.CO;2-B](https://doi.org/10.1002/1099-1085(200011/12)14:16/17<2959:AID-HYP129>3.0.CO;2-B)
- Travis, J. M. J. (2003). Climate change and habitat destruction: A deadly anthropogenic cocktail. *Proceedings of the Royal Society of London. Series B: Biological Sciences*, 270(1514), 467–473. <https://doi.org/10.1098/rspb.2002.2246>
- Walsh, R. P. D., & Newbery, D. M. (1999). The ecoclimatology of Danum, Sabah, in the context of the world's rainforest regions, with particular reference to dry periods and their impact. *Philosophical Transactions of the Royal Society of London. Series B: Biological Sciences*, 354(1391), 1869–1883. <https://doi.org/10.1098/rstb.1999.0528>
- Williams-Linera, G. (1990). Vegetation structure and environmental conditions of forest edges in Panama. *The Journal of Ecology*, 78(2), 356–373. <https://doi.org/10.2307/2261117>
- Williamson, J., Luke, S. H., Heroín, H., Vairappan, C. S., Slade, E. M., & Struebig, M. J. (2020). Riparian microclimates. *Zenodo*, <https://doi.org/10.5281/zenodo.4000207>
- Zellweger, F., De Frenne, P., Lenoir, J., Rocchini, D., & Coomes, D. (2019). Advances in microclimate ecology arising from remote sensing. *Trends in Ecology & Evolution*, 34(4), 327–341. <https://doi.org/10.1016/j.tree.2018.12.012>
- Zimbres, B., Peres, C. A., & Machado, R. B. (2017). Terrestrial mammal responses to habitat structure and quality of remnant riparian forests in an Amazonian cattle-ranching landscape. *Biological Conservation*, 206, 283–292. <https://doi.org/10.1016/j.biocon.2016.11.033>

## SUPPORTING INFORMATION

Additional supporting information may be found online in the Supporting Information section.

**How to cite this article:** Williamson J, Slade EM, Luke SH, et al. Riparian buffers act as microclimatic refugia in oil palm landscapes. *J Appl Ecol*. 2020;00:1–12. <https://doi.org/10.1111/1365-2664.13784>